energies

MDPI

Article

Tribological Performance of Biomass-Derived Bio-Alcohol and Bio-Ketone Fuels

Omid Doustdar, Soheil Zeraati-Rezaei, Jose Martin Herreros, Athanasios Tsolakis *, Karl D. Dearn and Miroslaw Lech Wyszynski

Department of Mechanical Engineering, School of Engineering, University of Birmingham, Birmingham B15 2TT, UK; o.doustdar@bham.ac.uk (O.D.); s.zeraatirezaei@bham.ac.uk (S.Z.-R.); j.herreros@bham.ac.uk (J.M.H.); k.d.dearn@bham.ac.uk (K.D.D.); m.l.wyszynski@bham.ac.uk (M.L.W.)
* Correspondence: a.tsolakis@bham.ac.uk

Abstract: This study relates to developing future alternative fuels and focuses on the effects of a fuel's molecular structure on its properties and performance in advanced propulsion systems. The tribological performance of various biomass-derived oxygenated alternative fuels, including butanol, pentanol, cyclopentanol, cyclopentanone, and gasoline and their blends with diesel, was investigated. Lubricity tests were conducted using a high-frequency reciprocating rig (HFRR). Cyclopentanone-diesel and cyclopentanol-diesel blends result in smaller wear scar sizes compared to using their neat forms. A lower steel disc contaminated with the alternative fuels during the HFRR tests resulted in worn surface roughness values lower than those of the neat diesel by up to 20%. It is believed that these reductions are mainly due to the presence of the hydroxyl group and the carbonyl group in alcohols and ketones, respectively, which make them more polar and consequently helps the formation of the protective lubrication film on the worn moving surfaces during the sliding process. Overall, the results from this study indicate that environmentally friendly cyclopentanol and cyclopentanone are practical and efficient fuel candidates for future advanced propulsion systems.

Keywords: bio-alcohol; bio-ketone; lubricity; tribology; HFRR

Citation: Doustdar, O.; Zeraati-Rezaei, S.; Herreros, J.M.; Tsolakis, A.; Dearn, K.D.; Wyszynski, M.L. Tribological Performance of Biomass-Derived Bio-Alcohol and Bio-Ketone Fuels. *Energies* **2021**, *14*, 5331. https://doi.org/10.3390/en14175331

Academic Editors: Robert H. Beach and Attilio Converti

Received: 26 July 2021
Accepted: 24 August 2021
Published: 27 August 2021

1. Introduction

Integrating alternative fuels with advanced combustion and aftertreatment systems in various propulsion systems, including electric vehicles [1], will improve vehicles' fuel economy and mitigate emissions formation and their environmental impact [2]. Recently, advanced combustion strategies such as gasoline compression ignition (GCI) have shown great potential for future internal combustion engines with higher efficiency and lower fuel consumption compared with using gasoline spark ignition (SI) [2,3]. A low cetane number of gasoline-like fuels (such as bio-alcohols and bio-ketones) prolongs the ignition delay in GCI engines, improving the local air-fuel mixing and resulting in significantly lower particle and NO_x emissions [2,4]. Most importantly, the required aftertreatment system for these engines will be more straightforward as the focus shifts to controlling carbon monoxide (CO) and hydrocarbon (HC) [2]. Moreover, GCI hybrid technology is expected to have significantly lower well-to-wheel greenhouse gas emissions (by up to 43%) than unhybridised GCI [5].

As next-generation promising alternative fuels, some bio-alcohols and bio-ketones are produced from biomass-derived waste or lignocellulosic materials, such as agricultural wastes, forest residues, sewage and municipal wastes and used oils [6,7]. Their life cycle greenhouse gas emissions can be considerably lower than that of conventional fuels, depending on production [8,9]. Alcohols with three or more carbons (such as butanol and pentanol) compared with short-chain alcohols (such as methanol and ethanol); have better blending stability with conventional fuels, higher density, and a higher calorific value [6,9].

Furthermore, long-chain alcohols have a more favourable cold filter plugging point, pour point, cloud point and freezing point [10,11].

In addition to the aforementioned straight-chain alcohols, some cyclic alcohols (e.g., cyclopentanol) and cyclic ketones (e.g., cyclopentanone) seem to be promising candidates for blending with conventional fuels. Producing cyclopentanol and cyclopentanone is more cost-effective than some straight-chain alcohols, such as butanol [12]. Butanol is conventionally produced via the hydrolysation of lignocellulose (mainly composed of cellulose, hemicellulose and lignin) into sugar, and then through a complicated biochemical process into the end product [13]. Cyclopentanol and cyclopentanone are produced by the hydrolysation of lignocellulose into furfurals and the hydrogenation into the end products. Therefore, they are regarded as highly environmentally friendly alternative fuels, with great economic potential for practical use [12,14].

In addition to the energy and ecological benefits of the low-cetane-number alternative fuels, these fuels can be matched with the current and future engines to enable a faster transition away from conventional fuels [15]. The molecular structure of fuels can affect engine durability, efficiency and emissions [3,16]. In modern engines, a direct injection (DI) of fuel into the combustion chamber with a high pressure enhances fuel atomisation for a better air-fuel mixing, a faster evaporation and a more efficient combustion process [17]. Fuel injection system components (e.g., injector and pump) need fuels with a high lubricity to prevent wear and corrosion issues [18–21]. Moreover, poor lubricity can cause energy losses within an engine due to friction. Many failures in the automotive and aviation industries due to the misfunctioning of fuelling systems led to the detailed investigation of fuel lubricity [18,22]. In the molecular structure of fuels, sulphur, a high unsaturation degree, a long alkyl chain length, polyaromatic, nitrogen, polar oxygen-containing compounds and fatty acid contents enhance fuel lubricity [20]. Fuel refining processes, such as desulphurisation for meeting the regulatory standards, decrease the fuel lubricity. The tribological performance can be categorised into boundary lubrication, mixed lubrication and hydrodynamic lubrication. Fuel lubrication is usually visible at the boundary lubrication regime, where lubricated films are thin and require the formation of a protective tribofilm to eliminate the frictional forces and surface wear [23].

The bio-alcohols and bio-ketones mentioned above are well defined in their engine combustion and emissions characteristics [6,7,14,24], but not in their tribological performance. The current work comprehensively investigates the effects of diesel blending with bio-alcohols (i.e., butanol, pentanol and cyclopentanol) and a bio-ketone (i.e., cyclopentanone) with different molecular structures (C_4 and C_5) and gasoline-diesel blends on the fuels' properties and tribological performance. The neat form of these fuels was also investigated. EN ISO 12156-1:2016 [25], a standard test method for the High-Frequency Reciprocating Rig (HFRR), was used to assess the lubricity of the neat fuels and blends. After the lubricity tests, the friction properties, wear scar size, deposits and surface roughness of the tested specimens were further analysed using a 3D microscope, a scanning electron microscope (SEM) and Energy-dispersive X-ray spectroscopy (EDS).

2. Materials and Methods

2.1. Fuels

Butanol (B), pentanol (P), cyclopentanol (CP), cyclopentanone (CPK) and gasoline (G) fuels and their blends with diesel (D) were studied, considering diesel fuel as the reference. No other additives, such as lubricity or cetane enhancers, were incorporated in the neat fuels and blends. Shell Global Solutions UK supplied the European ultra-low sulphur diesel (specification EN 590) and European gasoline (G) (specification EN 228). The butanol, pentanol, cyclopentanol and cyclopentanone were purchased from Sigma Aldrich UK. They were blended with diesel only at 20% and 40% ratios (volume basis-% v/v) because higher proportions significantly deteriorate the self-ignition properties in an engine. However, the GCI technique case study analysed the gasoline-diesel blends with a ratio (% v/v) of 20%, 40%, 60% and 80%.

2.2. Fuel Physicochemical Properties

Fuel viscosity was analysed with an Ultra Shear Viscometer (USV-PCS Instruments Ltd, London, UK). A maximum bubble pressure method was used for the surface tension tests with a Sita Proline T15 Tension meter at a constant temperature of 25 °C. Lower heating value measurements were carried out with an oxygen bomb in a C200 calorimeter (IKA® England Ltd, Oxford, UK).

2.3. Analysis of Lubrication Mechanisms

The lubricity of the fuels was measured by the HFRR supplied by PCS Instruments, UK. The testing procedures in the HFRR were carried out following the standard EN ISO 12156-1 [25]. A gasoline PTFE conversion kit was used to prevent the excessive evaporation and contamination of the fuels. A 15 mL sample of fuels was used throughout the tests to minimise any uncertainty during the possible fuel evaporation. During the HFRR test, the standard upper specimen (a steel ball with 6 mm diameter) and the lower specimen (a steel disc with 10 mm diameter) were submerged in the tested sample with a load of 200 g. Due to the standard, the test duration was 75 min, with a stroke of 1 mm at a frequency of 50 Hz. HFRR reported the friction coefficient and the wear scar diameter (WSD). The wear scar generated with HFRR was measured optically using the microscope Meiji Techno, Somerset, UK, with a 100× magnification lens, by measuring the length of wear scar on the tested ball in the X and Y directions. The lower disc test sample's surface was then analysed using a 10× magnification lens on a G5 Infinite Focus optical 3D microscope (Alicona Ltd., Kent, UK). This methodology characterises the average wear scar depth and the surface roughness of the wear track on the lower disc specimen. The chemical composition on the lower disc test samples' surface was also analysed using SEM-EDS JCM-6000Plus NeoScope Benchtop, JEOL, UK, Ltd. It should be mentioned that all of the experimental data for the fuel characterisation and lubricity studies in this paper are the average of at least three measurements. The standard deviation of measurements was calculated and monitored to confirm the repeatability.

3. Results

3.1. Fuel Physicochemical Properties

Tables 1 and 2 show that a lower heating value, viscosity and surface tension indicated a direct relationship between the blending concentration of the alternative fuels with diesel. Based on the results, the surface tension increased with viscosity and density when straight-chain alcohols (such as butanol and pentanol) were used in the blend, in contrast to the case of cyclopentanol and cyclopentanone, which can be due to their polar cyclic structure. Based on the EN 590 standard, the diesel fuel viscosity should be more than two cSt. Therefore, cyclopentanol, cyclopentanone, pentanol, butanol and gasoline blended with diesel fuel with different concentrations (except G80) can pass the required viscosity limit to be used in CI engines [11]. The lowest viscosity value was for the neat cyclopentanone, and was due to its double bonds [26].

Table 1. Physical and chemical properties of neat tested fuels.

Property	Method	Diesel	Gasoline	Butanol	Pentanol	Cyclopentanol	Cyclopentanone
Molecular formula		$C_{12}H_{22}$	~$C_{5.88}H_{11.06}$	C_4H_9OH	$C_5H_{11}OH$	C_5H_9OH	C_5H_8O
Molecular weight (kg·kmol^{-1})		166.30	81.78	74.11	88.15	86.13	84.12
Density, 15 °C (kg·m^{-3}) [a]	EN ISO 3675	834.8	746.6	811.5	814.8	949.0	948.7
Kinematic viscosity, 40 °C (cSt) [b]	EN ISO 3104	2.627 ± 0.05	0.80 ± 0.05	2.17 ± 0.05	2.74 ± 0.05	2.84 ± 0.05	1.30 ± 0.05
Lower heating value (MJ·kg^{-1}) [c]	ASTM D240-02	45.97 ± 0.5	41.66 ± 0.5	33.81 ± 0.5	34.65 ± 0.5	35.96 ± 0.5	36.43 ± 0.5
Heat of evaporation (kJ·kg^{-1}) [d]		270–350	373	581.4	308.05	-	433
Lubricity at 60 °C (µm) [e]	EN ISO 12156-1	462.5 ± 5.5	676 ± 10.0	628 ± 6.0	579 ± 3.0	452 ± 5.0	521 ± 3.0
Surface Tension, 25 °C (mN·m^{-1}) [f]	ASTM D971	26.07 ± 0.2	18.92 ± 0.5	23.05 ± 0.6	24.02 ± 0.4	31.35 ± 0.4	30.45 ± 0.4
Cetane number [g]	ASTM D6890	53	-	15.92	18.2	9.8	9
Carbon (wt%)		86.44	83.12	64.86	68.13	69.82	70.28
Hydrogen (wt%)		13.56	13.4	13.51	13.72	11.61	10.70
Oxygen (wt%)		0	3.48	21.62	18.15	18.57	19.02
H/C ratio		1.83	1.88	2.50	2.40	2.00	1.80
Boiling point (°C) [h]		180–360	35–200	117.4	137.9	140.4	131
CFPP (°C) [h]	EN 116	−20	-	−41.7	−47.02	−47.09	−46.47

[a, d, g, h] Provided by fuel suppliers or taken from the literature [10,24,27]; [b, c, f] Measured and compared with the literature [6,10]; [e] Measured.

Table 2. Physical and chemical properties of blended tested fuels.

Property	Method	B20	B40	P20	P40	CP20	CP40	CPK20	CPK40	G20	G40	G60	G80
Density at 15 °C (kg·m^{-3}) [a]	EN ISO 3675	830.14	830.80	857.64	857.84	825.48	826.80	880.48	880.88	817.2	799.5	781.9	764.2
Kinematic viscosity, 40 °C (cSt) [b]	EN ISO 3104	2.27 ± 0.05	2.60 ± 0.05	2.75 ± 0.05	2.35 ± 0.05	2.16 ± 0.05	2.65 ± 0.05	2.78 ± 0.05	2.11 ± 0.05	2.15 ± 0.05	2.10 ± 0.05	2.00 ± 0.05	1.80 ± 0.05
Lower heating value (MJ·kg^{-1}) [c]	ASTM D240-02	43.54 ± 0.5	43.99 ± 0.5	43.97 ± 0.5	43.86 ± 0.5	41.11 ± 0.5	42.01 ± 0.5	41.97 ± 0.5	41.76 ± 0.5	45.11 ± 0.5	44.25 ± 0.5	43.38 ± 0.5	42.52 ± 0.5
Lubricity (µm) [d]	EN ISO 12156-1	570 ± 10.0	562 ± 2.0	480 ± 6.0	425 ± 5.0	592 ± 4.0	576 ± 1.0	465 ± 5.0	441.5 ± 1.0	469.5 ± 3.5	474 ± 3.0	484 ± 6.0	497 ± 5.0
Surface Tension, 25 °C (mN.m^{-1}) [e]		25.48 ± 0.4	24.78 ± 0.4	26.30 ± 0.3	26.30 ± 0.3	24.48 ± 0.3	24.51 ± 0.3	26.85 ± 0.4	26.55 ± 0.4	24.90 ± 0.5	24.00 ± 0.4	22.00 ± 0.4	20.50 ± 0.4
Carbon (wt%)		82.39	83.03	82.92	83.28	77.93	79.25	79.89	80.56	-	-	-	-
Hydrogen (wt%)		13.39	13.41	12.97	12.51	13.44	13.49	12.68	11.84	-	-	-	-
Oxygen (wt%)		4.22	3.56	4.11	4.21	8.63	7.26	7.43	7.60	-	-	-	-
CFPP (°C) [f]	EN 116	−19.99	−20.06	−20.07	−20.03	−20.01	−20.86	−20.92	−20.56	-	-	-	-

[a] Calculated; [b, c, e] Measured and compared with the literature [6,10]; [d] Measured; [f] Provided by fuel suppliers or taken from the literature [10,24,27].

3.2. Friction and Wear Resistance

Figure 1a,b presents the average friction coefficient and wear scar diameter (WSD) for the tested fuels. The friction coefficient of the neat fuels as shown in Figure 1a is in the following order: gasoline > butanol > pentanol > cyclopentanol > cyclopentanone > diesel. The friction coefficient of the neat gasoline is 50% higher than that of the neat diesel. It can be observed that the neat cyclopentanone as a ketone shows a lower friction coefficient (only 20% higher than diesel) than the rest of the alternative fuels. Generally, in low sulphur fuels, as is the case here, there is no correlation between viscosity and lubricity. For example, double bonds in fuels (cyclopentanone) improve the lubricity values, but the viscosity worsens [26].

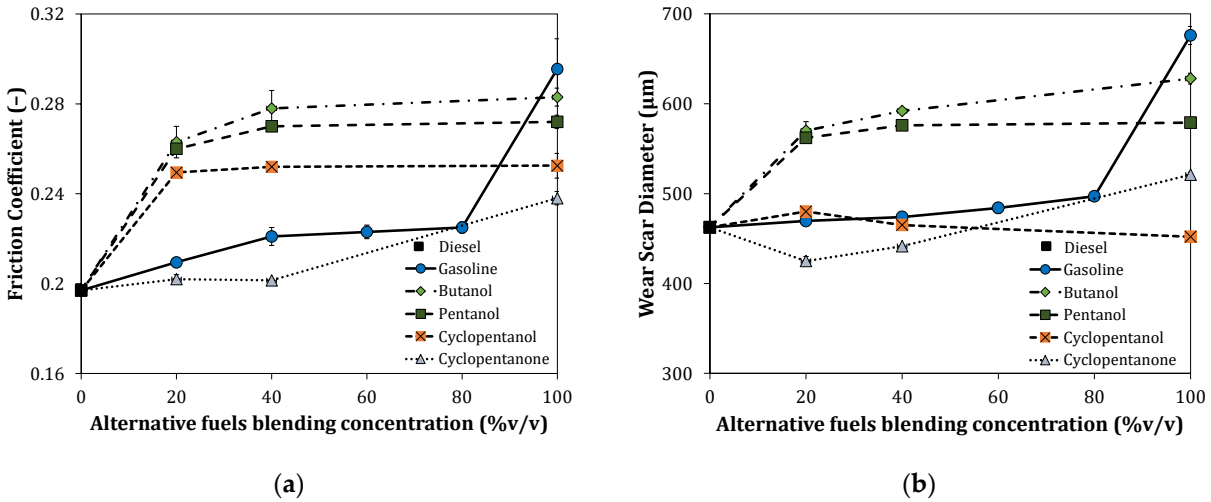

Figure 1. (**a**) Friction coefficient and (**b**) wear scar diameter of the neat tested fuels and their blends with diesel (i.e., 0: neat diesel, 100: neat alternative fuel).

Compared with the neat alternative fuels, the presence of diesel in the blended fuels enhanced the frictional properties, with a reduction in the average friction coefficient. The friction coefficient of butanol–diesel blends increased from 0.263 to 0.278 by increasing the butanol concentration from 20% to 40%. The increase of the friction coefficient for pentanol blends was from 0.260 to 0.270; cyclopentanol blends increased from 0.249 to 0.252. However, increasing the concentration of cyclopentanone from 20% to 40% did not significantly affect the friction coefficient (constant around 0.202). Moreover, gasoline concentrations of 20%, 40%, 60%, and 80% blended with diesel increased the friction coefficient to 0.2095, 0.221, 0.223 and 0.225. This means that the saturation of gasoline occurs at higher gasoline concentrations in diesel.

Figure 1b shows that cyclopentanol has the smallest wear scar diameter (WSD) among the studied fuels in the neat form (approximately 4% lower than diesel), probably due to its higher viscosity [17]. The order of the oxygenated moieties in the neat fuels for enhancing the wear resistance (lower WSD value) is cyclopentanol > cyclopentanone > pentanol > butanol. Knothe et al. [28] stated that in the molecular structure of fuels, the presence of polarity-imparting heteroatom, preferably oxygen, with the oxygen moiety's nature having a significant role and/or a carbon chain of sufficient length, increases viscosity and lubricity. Additionally, the presence of oxygen as a double bond is recognised as beneficial in improving lubricity [29].

The gasoline–diesel blend results show that adding 20 vol% gasoline to diesel increased the WSD by 1.5%. This is increased to 2.5%, 4.7% and 7.5% with 40%, 60% and 80% gasoline blended with diesel, respectively. By adding 20 vol% of the oxygenated compounds to diesel, the WSD increases by 23% for the butanol–diesel blend, 21% for the pentanol–diesel blend and 3% for the cyclopentanol–diesel blend. However, the cyclopentanone blended with diesel shows the smallest WSD value among all the fuels (even up to

8% less than neat diesel). This reduction in wear is due to the higher degree of unsaturation (i.e., the cyclic molecular structure and the double bond oxygen in its structure), making a protective lubrication film, with the attraction between the partially positive-charged metal surface and the lone pair electron on the oxygen atom [29].

Additionally, only at specific oxygen concentrations in the tested samples, friction decreased due to the formation of protective oxide layers with anti-adhesive properties. Reduced friction could be the main reason for having the highest WSD of butanol with the highest oxygen content compared to other fuels. The presented results indicate that cyclic alcohols–diesel and cyclic ketone–diesel blends would be more suitable for high-pressure fuel injection systems in modern advanced engines. This chemistry will improve the components' efficiency, longevity and reliability within the fuel delivery systems [18].

In general, the lubricious molecules improve lubricity by making solid interactions between the moieties and negatively charged contacting metallic surfaces, enhancing tribo-film growth and preventing metallic surface contact, leading to a lower friction and surface wear [21,23]. It is confirmed that an increase in the chain length and the presence of the unsaturated compounds improve the lubricity of alcohols [19]. For example, the OH and C = O groups in alcohols and ketones make the tested samples more effective as wear protectors [21,28]. In addition, increasing the molecular weight of the straight-chain alcohols increases the polarity, chain-length, viscosity and boiling point, leading to lubricity improvement [11,20].

3.3. Wear and Lubrication Mechanisms

The wear scars on the upper and lower specimens (ball and disc) were investigated in detail using SEM and EDS. For example, SEM and topography micrographs of the discs tested in the neat fuels are presented in Figure 2. SEM images of the lower specimen were presented in two different resolutions (i.e., full image of the worn disc: ×70, 200 µm, and zoomed image for topography analysis: ×400, 50 µm). There is a partial corrosion field at the junction of the worn and non-worn surfaces, particularly in the samples where the fuel molecules adsorbed on the wear surface to assist with the lubrication. It is believed that the magnetic media during the sliding and friction process led to the formation of a lubrication boundary. The optical observation of the disc specimens tested in various oxygenated compounds displays a trend similar to that of the scar size results. The specimen tested with the neat gasoline had a large wear scar with lots of abrasive, dense grooves and material losses in the wear area due to the poor lubricity and higher friction coefficient of gasoline. This catalysed process can be due to the formation of different acids during the sliding process, which increases the corrosive wear. The close observation of the worn surfaces shows that samples with smaller wear scar sizes have a smooth surface with little and slight furrows.

Some slight, dense furrows and few pits can be seen in the SEM images (i.e., ×400, 50 µm) for the lower specimen. Fuel pits are like tiny dots, which can be seen in the images, and parallel furrows are presented clearly as lines. Slight furrows appeared on cyclopentanone and cyclopentanol with smaller wear scar sizes. The formation of the protective lubrication film, composed of adsorbed and tribo-reacted organics on worn surfaces during the lubricity test, have minimised the wear damage and created small furrows [30]. These smooth worn surfaces in the SEM images are due to the strong polarity of the compounds, which leads to the creation of a robust lubrication regime and protects the metal surface from wear. A large amount of ferrite in poor lubricity samples around the carbide particles is due to the carbide particles' detachment from the surface and the formation of delamination (e.g., for gasoline, butanol and pentanol). These micrographs show a surface damage that is in good agreement with other measured tribological behaviours.

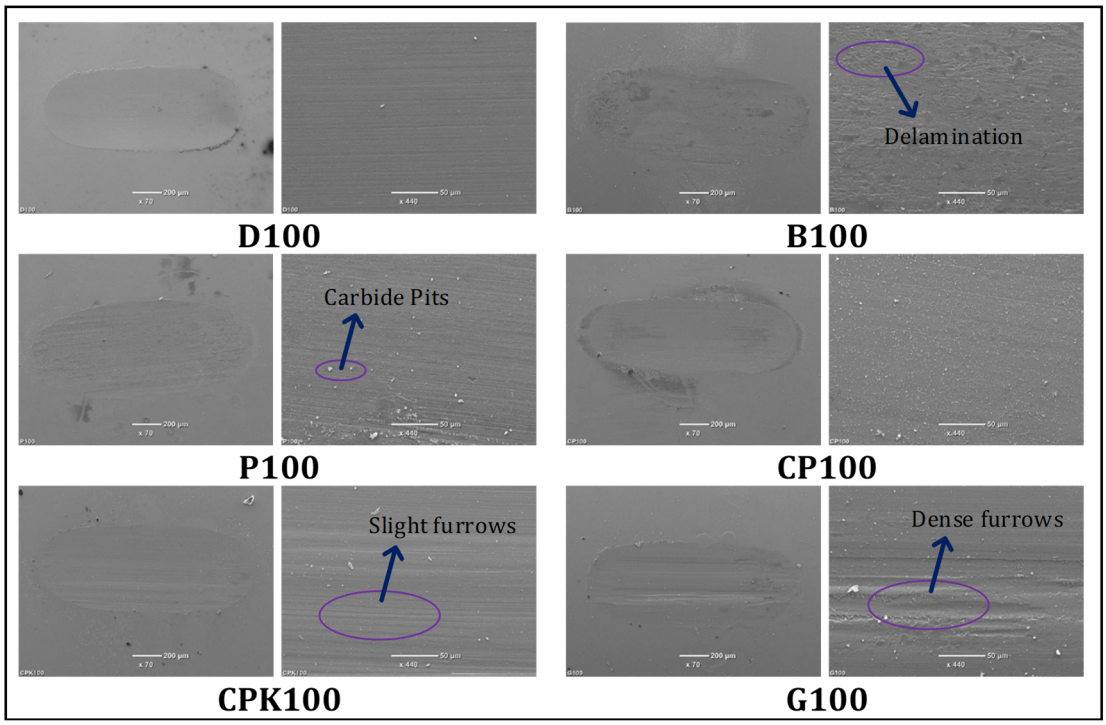

Figure 2. SEM and topography micrographs of a disc tested in different fuels.

The element contents of the worn surface analysis with EDS confirmed the findings of the lubrication investigation. The EDS analysis indicated that the deposits formed on the disc's surface were mainly iron (Fe), carbon and oxygen. These are the oxidation reaction products that occurred during the sliding process between the ball and the disc. Fuel hydrocarbons' adsorption and chemical reaction formed carbon when sliding the ball over the disc in the HFRR. The carbon content is more visible on the edge of the wear scar surface than on the middle area [31]. In the SEM images of the surfaces that show severe damages and grooves, such as the tested gasoline fuel, the carbon content significantly increased, and the Fe content decreased. The increase of carbon is expressed as organic deposits, including oxides on the worn surfaces. In addition to the corrosion effect, the lubrication film caused a reduction of the Fe content in the sampling area. These illustrations confirm the result of the friction coefficient and WSD values from the HFRR.

During the HFRR tests, the materials were transferred between samples and then oxidised and detached as a fine brown powder (either as Fe_2O_3 (hematite) or $Fe_2O_3 \cdot nH_2O$ (hydrohermatite)) [32]. The oxidation process in sliding materials is seen in the tested fuels due to the presence of oxygen associated with the formation of inorganic oxides (Fe_3O_4 and Fe_2O_3), which help create a protective lubrication film and reduce the dimensions of the worn surface [33–35].

3.4. Surface Topography

The lower disc sample wear scar depth values created during the lubricity test can be seen in Figure 3a. This figure shows the average of at least three profile measurements perpendicular to the sliding direction. The wear scar depth profile follows the same pattern for the wear scar diameter for most tested samples. For the neat fuels, the wear scar diameters are higher for butanol > pentanol > gasoline > cyclopentanone > cyclopentanol. The wear scar depths are higher for butanol > pentanol > cyclopentanone > gasoline > cyclopentanol. The depth of the wear scar for diesel is 10.2281 µm, decreasing by approximately 38% for cyclopentanol and 22% for cyclopentanone. These trends increased by 13% for butanol and 5% for pentanol, compared with diesel. The addition of 20 vol% of pentanol, butanol and cyclopentanone to diesel shows the same trend for scar depth,

reducing by 9% with the addition of 20 vol% of cyclopentanone to diesel. Gasoline and cyclopentanol had a small difference. In contrast, with the addition of 40% (% v/v) of fuels to the diesel, only the cyclopentanol patterns for depth and diameter remained the same. This difference is due, in some cases, to the deformation of the upper specimen ball during lubricity testing, as the steel material is removed, especially in less lubricious fuels like gasoline.

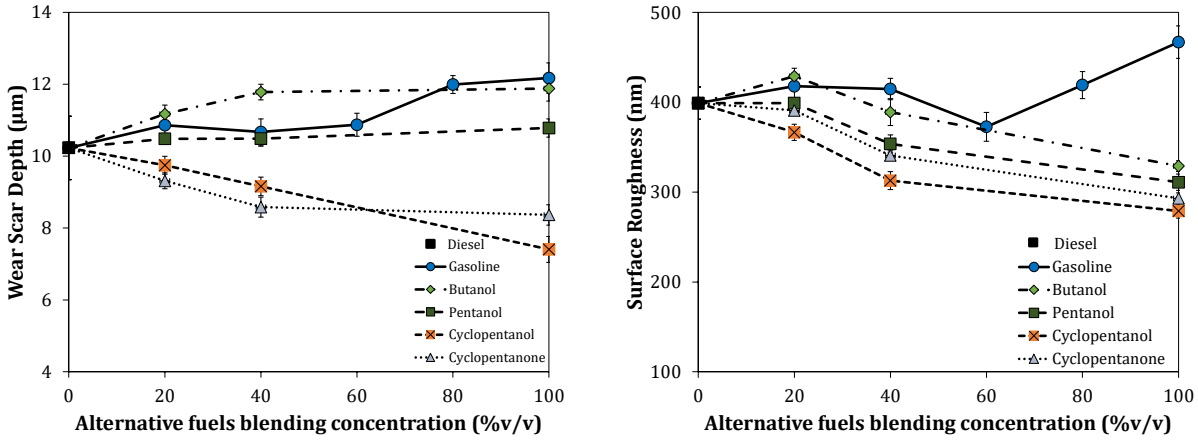

Figure 3. (**a**) Wear scar depth and (**b**) surface roughness of the disc tested in the neat fuels and their blends with diesel (i.e., 0: neat diesel, 100: neat alternative fuel).

The surface roughness for all the tested sample discs is shown in Figure 3b. These results confirm the findings of the SEM studies. An increase in the oxide layer thickness and metallic oxide wear particles increases the wear diameter, depth and surface roughness [20]. All tested samples' surface roughness is less than for diesel, except for neat gasoline and its blends and 20% butanol. This lower surface roughness could be due to the oxide layer discussed in Section 3.3. In most cases, diesel's wear scar diameter and depth are lower than for other fuels, but its surface roughness is higher, which could be due to impurities in its structure.

In summary, the worn surface analysis by SEM, EDS and Alicona confirms the HFRR tests findings. In general, cyclopentanol and cyclopentanone's wear scar diameter, scar depth and worn surface roughness show a slight enhancement in lubricity compared with diesel. Pentanol shows a better tribological performance than butanol. The optimum fuels in minimising wear are CP20 and CPK20, which have a lower wear scar diameter and depth, applicable roughness and a less corroded area. They would be suitable for an engine's fuelling system, with great potential for advanced combustion techniques due to the low cetane number of blends [27].

4. Conclusions

The tribological performance of butanol, pentanol, cyclopentanol, cyclopentanone, gasoline and their blends with diesel was comprehensively investigated. Fuels with cyclic structures have better lubricating characteristics than other alternative fuels due to the significant effect of the functional group's polarity and the higher degree of unsaturation when forming a lubrication film on the sliding areas. Regarding the wear scar diameter and depth, cyclopentanone and cyclopentanol show a better lubrication performance than the others. The presence of oxygen and the cyclic structure help form a protective lubrication film and reduce the wear scar dimensions. Pentanol with a longer carbon chain length shows better lubricity than butanol. The influence of the molecular structure of oxygenated compounds blended with diesel on enhancing lubricity can be ranked as follows: cyclic hydroxyl > cyclic carbonyl > straight hydroxyl. The addition of 20% of cyclopentanone

to diesel shows the best lubrication performance due to the solid protective lubrication film formation on the moving worn surfaces. The significant dipole moment, due to the carbonyl group in the ketones having electronegative oxygen, could be a reason. When using different blends of fuels, surface roughness has the same trend as the wear scar sizes for the neat fuels. All tested oxygenated alternative fuels in the neat form show a lower roughness than the neat diesel, which is hypothesised to be due to the protective oxide layer. All of the characterisation methods confirm that manipulating the molecular structure of the fuel affects the lubrication and tribological mechanics. This research presents the ecological benefits of biomass-derived bio-alcohols and bio-ketones for a high-pressure fuelling system for low emission vehicles.

Author Contributions: Conceptualisation, O.D., S.Z.-R., J.M.H. and A.T.; methodology, O.D.; formal analysis, O.D.; investigation, O.D.; resources, A.T. and K.D.D.; data curation, O.D.; writing—original draft preparation, O.D.; writing—review and editing, O.D., S.Z.-R., J.M.H., A.T. and K.D.D.; visualisation, O.D.; supervision, A.T. and M.L.W.; project administration, J.M.H. and A.T.; funding acquisition, A.T., K.D.D. and M.L.W. All authors have read and agreed to the published version of the manuscript.

Funding: This research was funded by EPSRC with the FACE project (EPSRC Ref: EP/P03117X/1).

Institutional Review Board Statement: Not applicable.

Informed Consent Statement: Not applicable.

Data Availability Statement: Not applicable.

Acknowledgments: EPSRC is acknowledged for supporting this work through the FACE project (EPSRC Ref: EP/P03117X/1). Special appreciation is due to the University of Birmingham and the European Union's Horizon 2020, the Knocky projects (grant agreement No 691232-Knocky-H2020-MSCA-RISE 2015) for a PhD scholarship and a financial grant to Omid Doustdar. We also thank the Advanced Manufacturing Technology Centre, and particularly Vahid Nasrollahi, for helping in the use of the Alicona Infinite Focus system. Finally, the authors would like to express their gratitude to Shell Global Solutions UK for providing diesel and gasoline fuels for this work.

Conflicts of Interest: The authors declare no conflict of interest.

Abbreviations

B	Butanol
B20	Butanol 20% + Diesel 80% (v/v)
B40	Butanol 40% + Diesel 60% (v/v)
C	Atomic carbon
CFPP	Cold filter plugging point
CH_3OH	Methanol
C_2H_5OH	Ethanol
C_4H_9OH	Butanol
$C_5H_{11}OH$	Pentanol
CI	Compression ignition
CP	Cyclopentanol
CP20	Cyclopentanol 20% + Diesel 80% (v/v)
CP40	Cyclopentanol 40% + Diesel 60% (v/v)
CPK	Cyclopentanone
CPK20	Cyclopentanone 20% + Diesel 80% (v/v)
CPK40	Cyclopentanone 40% + Diesel 60% (v/v)
D	Diesel
EDS	Energy dispersive spectrometer
EN	European Standards
EU	European Union
G	Gasoline
G20	Gasoline 20% + Diesel 80% (v/v)
G40	Gasoline 40% + Diesel 60% (v/v)
G60	Gasoline 60% + Diesel 40% (v/v)

G80	Gasoline 80% + Diesel 20% (*v*/*v*)
GCI	Gasoline compression ignition
H	Atomic hydrogen
HCF	Humidity correction factor
HFRR	High-frequency reciprocating rig
ISO	International Standard Organization
O	Atomic oxygen
O_2	Oxygen
OH	Hydroxyl radicals
P	Pentanol
P20	Pentanol 20% + Diesel 80% (*v*/*v*)
SEM	Scanning electron microscope
SI	Spark ignition
ULSD	Ultralow sulphur diesel
WSD	Wear scar diameter

References

1. Kalghatgi, G. Is it really the end of internal combustion engines and petroleum in transport? *Appl. Energy* **2018**, *225*, 965–974. [CrossRef]
2. Leach, F.; Kalghatgi, G.; Stone, R.; Miles, P. The scope for improving the efficiency and environmental impact of internal combustion engines. *Transp. Eng.* **2020**, *1*, 100005. [CrossRef]
3. Kalghatgi, G. Development of Fuel/Engine Systems—The Way Forward to Sustainable Transport. *Engineering* **2019**, *5*, 510–518. [CrossRef]
4. Zeraati-Rezaei, S.; Al-Qahtani, Y.; Herreros, J.M.; Ma, X.; Xu, H. Experimental investigation of particle emissions from a Dieseline fuelled compression ignition engine. *Fuel* **2019**, *251*, 175–186. [CrossRef]
5. Abdul-Manan, A.F.N.; Won, H.-W.; Li, Y.; Sarathy, S.M.; Xie, X.; Amer, A.A. Bridging the gap in a resource and climate-constrained world with advanced gasoline compression-ignition hybrids. *Appl. Energy* **2020**, *267*, 114936. [CrossRef]
6. Rajesh Kumar, B.; Saravanan, S. Use of higher alcohol biofuels in diesel engines: A review. *Renew. Sustain. Energy Rev.* **2016**, *60*, 84–115. [CrossRef]
7. Pinzi, S.; Redel-Macías, M.D.; Carmona-Cabello, M.; Cubero, A.; Herreros, J.M.; Dorado, M.P. Influence of 1-butanol and 1-pentanol addition to diesel fuel on exhaust and noise emissions under stationary and transient conditions. *Fuel* **2021**, *301*, 121046. [CrossRef]
8. Sukjit, E.; Herreros, J.M.; Dearn, K.D.; García-Contreras, R.; Tsolakis, A. The effect of the addition of individual methyl esters on the combustion and emissions of ethanol and butanol -diesel blends. *Energy* **2012**, *42*, 364–374. [CrossRef]
9. Fernández-Rodríguez, D.; Lapuerta, M.; German, L. Progress in the Use of Biobutanol Blends in Diesel Engines. *Energies* **2021**, *14*, 3215. [CrossRef]
10. Lapuerta, M.; Rodríguez-Fernández, J.; Fernández-Rodríguez, D.; Patiño-Camino, R. Cold flow and filterability properties of n-butanol and ethanol blends with diesel and biodiesel fuels. *Fuel* **2018**, *224*, 552–559. [CrossRef]
11. Lapuerta, M.; García-Contreras, R.; Campos-Fernández, J.; Dorado, M.P. Stability, Lubricity, Viscosity, and Cold-Flow Properties of Alcohol−Diesel Blends. *Energy Fuels* **2010**, *24*, 4497–4502. [CrossRef]
12. Zhou, X.; Feng, Z.; Guo, W.; Liu, J.; Li, R.; Chen, R.; Huang, J. Hydrogenation and Hydrolysis of Furfural to Furfuryl Alcohol, Cyclopentanone, and Cyclopentanol with a Heterogeneous Copper Catalyst in Water. *Ind. Eng. Chem. Res.* **2019**, *58*, 3988–3993. [CrossRef]
13. Yan, K.; Wu, G.; Lafleur, T.; Jarvis, C. Production, properties and catalytic hydrogenation of furfural to fuel additives and value-added chemicals. *Renew. Sustain. Energy Rev.* **2014**, *38*, 663–676. [CrossRef]
14. Chen, H.; Su, X.; He, J.; Zhang, P.; Xu, H.; Zhou, C. Investigation on combustion characteristics of cyclopentanol/diesel fuel blends in an optical engine. *Renew. Energy* **2020**, *167*, 811–829. [CrossRef]
15. Kuszewski, H.; Jakubowski, M.; Jaworski, A.; Lubas, J.; Balawender, K. Effect of temperature on tribological properties of 1-butanol–diesel fuel blends–Preliminary experimental study using the HFRR method. *Fuel* **2021**, *296*, 120700. [CrossRef]
16. Hellier, P.; Talibi, M.; Eveleigh, A.; Ladommatos, N. An overview of the effects of fuel molecular structure on the combustion and emissions characteristics of compression ignition engines. *Proc. Inst. Mech. Eng. Part D J. Automob. Eng.* **2018**, *232*, 90–105. [CrossRef]
17. Sukjit, E.; Tongroon, M.; Chollacoop, N.; Yoshimura, Y.; Poapongsakorn, P.; Lapuerta, M.; Dearn, K.D. Improvement of the tribological behaviour of palm biodiesel via partial hydrogenation of unsaturated fatty acid methyl esters. *Wear* **2019**, *426*, 813–818. [CrossRef]
18. Dearn, K.D.; Moorcroft, H.; Sukjit, E.; Poapongsakorn, P.; Hu, E.Z.; Xu, Y.F.; Hu, X.G. The tribology of fructose derived biofuels for DISI gasoline engines. *Fuel* **2018**, *224*, 226–234. [CrossRef]
19. Sukjit, E.; Poapongsakorn, P.; Dearn, K.D.; Lapuerta, M.; Sánchez-Valdepeñas, J. Investigation of the lubrication properties and tribological mechanisms of oxygenated compounds. *Wear* **2017**, *376*, 836–842. [CrossRef]

20. Lapuerta, M.; Sánchez-Valdepeñas, J.; Sukjit, E. Effect of ambient humidity and hygroscopy on the lubricity of diesel fuels. *Wear* **2014**, *309*, 200–207. [CrossRef]
21. Lapuerta, M.; Garcia-Contreras, R.; Agudelo, J.R. Lubricity of Ethanol-Biodiesel-Diesel Fuel Blends. *Energy Fuels* **2009**, *24*, 6. [CrossRef]
22. Uchôa, I.M.A.; Deus, M.S.; Barros Neto, E.L. Formulation and tribological behavior of ultra-low sulfur diesel fuels microemulsified with glycerin. *Fuel* **2021**, *292*, 120257. [CrossRef]
23. Hong, F.T.; Alghamdi, N.M.; Bailey, A.S.; Khawajah, A.; Sarathy, S.M. Chemical and kinetic insights into fuel lubricity loss of low-sulfur diesel upon the addition of multiple oxygenated compounds. *Tribol. Int.* **2020**, *152*, 106559. [CrossRef]
24. Bao, X.; Jiang, Y.; Xu, H.; Wang, C.; Lattimore, T.; Tang, L. Laminar flame characteristics of cyclopentanone at elevated temperatures. *Appl. Energy* **2017**, *195*, 671–680. [CrossRef]
25. Publication, B.S. *Diesel Fuel—Assessment of Lubricity Using the High-Frequency Reciprocating Rig (HFRR)*; BS EN ISO 12156-1:2016; The British Standards Institution: London, UK, 2016.
26. Lapuerta, M.; Sánchez-Valdepeñas, J.; Bolonio, D.; Sukjit, E. Effect of fatty acid composition of methyl and ethyl esters on the lubricity at different humidities. *Fuel* **2016**, *184*, 202–210. [CrossRef]
27. Yanowitz, J.; Ratcliff, M.A.; McCormick, R.L.; Taylor, J.D.; Murphy, M.J. *Compendium of Experimental Cetane Numbers*; NREL/TP-5400-67585 United States 10.2172/1345058 NREL English; National Renewable Energy Lab. (NREL): Golden, CO, USA, 2017; 78p.
28. Knothe, G.; Steidley, K.R. Lubricity of Components of Biodiesel and Petrodiesel. The Origin of Biodiesel Lubricity. *Energy Fuel Am. Chem. Soc.* **2005**, *19*, 1192–1200. [CrossRef]
29. Kumar, N.; Varun; Chauhan, S. Analysis of tribological performance of biodiesel. *Proc. Inst. Mech. Eng. Part J J. Eng. Tribol.* **2014**, *228*, 797–807. [CrossRef]
30. Xu, Y.; Peng, Y.; Dearn, K.D.; Zheng, X.; Yao, L.; Hu, X. Synergistic lubricating behaviors of graphene and MoS2 dispersed in esterified bio-oil for steel/steel contact. *Wear* **2015**, *342*, 297–309. [CrossRef]
31. Sukjit, E.; Dearn, K.D. Enhancing the lubricity of an environmentally friendly Swedish diesel fuel MK1. *Wear* **2011**, *271*, 1772–1777. [CrossRef]
32. Arkoudeas, P.; Karonis, D.; Zannikos, F.; Lois, E. Lubricity assessment of gasoline fuels. *Fuel Process. Technol.* **2014**, *122*, 107–119. [CrossRef]
33. Maru, M.M.; Trommer, R.M.; Cavalcanti, K.F.; Figueiredo, E.S.; Silva, R.F.; Achete, C.A. The Stribeck curve as a suitable characterization method of the lubricity of biodiesel and diesel blends. *Energy* **2014**, *69*, 673–681. [CrossRef]
34. Xu, Y.; Wang, Q.; Hu, X.; Li, C.; Zhu, X. Characterization of the lubricity of bio-oil/diesel fuel blends by high frequency reciprocating test rig. *Energy* **2010**, *35*, 283–287. [CrossRef]
35. Habibullah, M.; Masjuki, H.H.; Kalam, M.A.; Zulkifli, N.W.M.; Masum, B.M.; Arslan, A.; Gulzar, M. Friction and wear characteristics of Calophyllum inophyllum biodiesel. *Ind. Crops Prod.* **2015**, *76*, 188–197. [CrossRef]